CILAMCE 2017
Florianópolis - Santa Catarina - Brazil

COMPUTATIONAL MODELLING OF THE LUBRICATED CONTACT BETWEEN ROUGH SURFACES IN ABAQUS

Marcus Vinicíus de Souza Ferraz

Flávia de Souza Bastos

marcus.ferraz@engenharia.ufjf.br

flavia.bastos@gmail.com

Universidade Federal de Juiz de Fora

Rua José Lourenço Kelmer, s/n - Bairro São Pedro - CEP: 36036-900 - Juiz de Fora - MG

Sara Del Vecchio

sara.vecchio@ifsudestemg.edu.br

Instituto Federal Sudeste de Minas Gerais

Rua Bernardo Mascarenhas, 1283 - Bairro Fábrica - CEP: 36080-001 - Juiz de Fora - MG

Abstract. *Tribology is an interdisciplinary science dedicated to the study of the phenomena related to wear, friction and lubrication between surfaces in relative motion. This paper consists in the modeling of rough surfaces in contact with a rigid plane, with a separating lubricant between them. The main objective has been to investigate how the lubrication influences contact conditions by means of numerical simulations through the fluid-structure interaction defined by the Arbitrary Lagrangian - Eulerian (ALE) method. At first, is realized a contextualization of the theme based on papers available in the literature, about different lubrication regimes. Then, the mathematical formulations that govern the lubrication process of contacts possibly found in tribological applications are presented, taking into account the Reynolds equations for modeling the film thickness for the lubrication regimes considered. The model was implemented in the program Abaqus®. The simulation is given by the displacement of this rigid plane in the normal direction of the main asperities, so that contact occurs. In addition, it seeks to establish a relative motion between such roughnesses and the plane. The results of an unlubricated model are compared with the results of a model lubricated in terms of tangential stress, normal stress and a ratio between the latter two. Therefore, significant differences in the distribution of stresses in some elements of the model and in the interface of contact between the analyzed pairs are identified through graphic results.*

Keywords: *Tribology, Lubrication, ALE method, Reynolds equation, Abaqus®*

1 INTRODUCTION

Tribology is defined as the field of science responsible for the study of friction, wear and lubrication of interactive surfaces in relative motion. Tribological contacts may be found in a variety of applications, including rolling elements bearings, hydraulic systems, biomechanic problems, such as the operation of the human hip joint and the human dental occlusal contact.

The main objective of lubrication is to control wear and reduce the friction between solid pairs in contact, since the latter mechanisms directly interfere in the tribological behavior of structures.

The contact between two flat and parallel surfaces occurs initially only at some points, due to the existence, even on carefully prepared surfaces, of roughness on a microscopic scale. As the normal load is increased, the surfaces become closer and a greater number of rough edges come into contact. These asperities are responsible for supporting the load and generate any frictional force. The knowledge of the topography of surfaces and an understanding of the interaction between them is essential for any study of friction, wear and lubrication.

According to Sanches (2006), numerical simulations are useful to evaluate the influence of different operational parameters and essential in the attempt to study the interfacial phenomena in a specially controlled way. Researches related to this field of study are becoming common due to the greater processing capacity of current computers and the demand for more precise results, capable of representing with more fidelity the existing phenomena. In many cases, however, there is a need to introduce many simplified hypotheses of the real problem to allow some form of mathematical modeling that leads to simpler solutions.

In the field of tribology, with emphasis on lubrication, few references and related research are found, but some approaches to investigate surface roughness influence on non-lubricated and lubricated contacts by means of the finite element analysis are studied by Lorentz (2013) and Hua et al. (1997).

However, the applications are more focused on the study and operation of bearings, as can be seen in the papers of Boman et al. (2004), Almqvist (2006), Kijima et al. (2009), Zhou et al. (2016), Khatri et al. (2016) and Quiñonez et al. (2016).

It has long been recognized that for many engineering problems, neither the Langrangian nor the Eulerian descriptions are well-suited because of their well-know intrinsic limitations (Boman, 2004).

The theoretical investigation of fluid structure interaction problems is complicated by the need of mixed description. While for the solid part the natural view is the material (Lagrangian) description, for the fluid it is the spatial (Eulerian) description. In the case of their combination some kind of mixed description (usually referred to as the arbitrary Lagrangian-Eulerian description) has to be used which brings additional nonlinearity into the resulting equations (Hron, 2006).

The motivation of this work is in the improvement of a preliminary model implemented by Bastos et al. (2017), which shows the contact between a barrier and a peak (making analogy to the rigid plane in contact with the roughness of the surface), and assumes that the plane is already in contact with the principal asperity (in this model there is no slip between the solid pairs). The geometry proposed for the realization of the simulation is represented by Fig. 1.

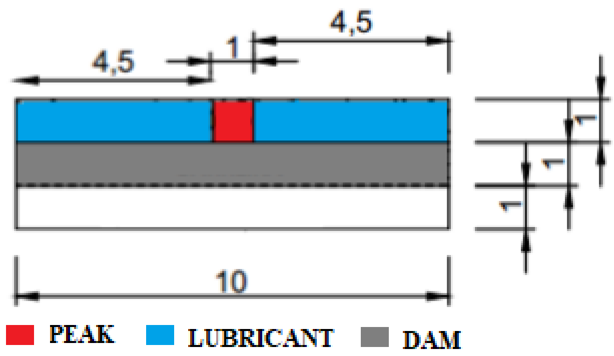

Figure 1: Preliminary model (dimensions in m) (Bastos et al., 2017)

This paper consists in the construction of a qualitative and hypothetical model that simulates the lubricated contact between the main asperities of any surface and a rigid plane in order to identify the contact pressure and the tangential pressure (τ_{xz}) resulting in the system due to the fluid-structure interaction characterized by the presence of the fluid film. This analysis is realized at some points of contact of asperities with the fluid (in the valleys), and the asperities with the rigid plane.

Thus, it is needed to understand the couplings between the lubricant fluid dynamics and the structural dynamics of surface roughness, particularly of the asperities in contact with the rigid plane, which makes modeling tribological applications an extremely delicate task.

At first, the mathematical formulations that govern the lubrication process of contacts possibly found in tribological applications are presented, taking into account the Reynolds equations and continuum descriptions for modeling the film thickness, besides the pressure-density relations describing compressibility, the pressure-viscosity relations and the boundary conditions for the lubrication regime considered - the mixed lubrication regime.

In this paper, the program used was Abaqus®, which contains an extensive library of elements that can model virtually any type of geometry.

Therefore, searches to compare the results of the model for two situations: the first one where the conditions of the mixed lubrication regime is not present and the second, characterized by a lubricated system, in order to verify how much the pressure coming from the confinement of the fluid influence on the surface interaction in question.

The contact occurs from the imposition of an initial condition of velocity, very small, as well as the speed responsible for the slip between the parts, so that the problem is almost static. An analysis of the model is realized considering the water $-$ incompressible fluid as lubricant (however, in the conditions which it is submitted it is assumed to be a compressible fluid).

2 ARBITRARY LAGRANGIAN - EULERIAN (ALE) METHOD

The complete resolution of a lubricated contact is a very challenging task because it implies the resolution of the coupled system composed of the equilibrium equations of the bodies in contact and the motion of the lubricant in the contact area. One of the major difficulties comes from the roughness of both surfaces in contact which significantly influence the lubricant flow (Boman et al., 2004).

The advantages and disadvantages of the ALE are related, respectively, to the ease and difficulty of modeling and analyzing the problem mathematically through the finite element method.

According to Qiu et al. (2011), in the Lagrangian description the movement of the continuum is specified as a function of the material coordinates and time. This is a particle description that is often applied in solid mechanics. In simulations using the Lagrangian formulation, the nodes of the Lagrangian mesh move together with the material. Therefore, the interface between two parts is precisely tracked and defined.

On the contrary, the Eulerian formulation is applied to the mechanics of fluids, and it is known as a spatial description. In this formulation, Boman et al. (2004) add that the material flows through the mesh and the initial mesh never gets distorted. However, some material which initially lies into the mesh can flow out of the domain and all information about that material is lost in such a case. In an ALE formulation, the mesh can be automatically handled by the

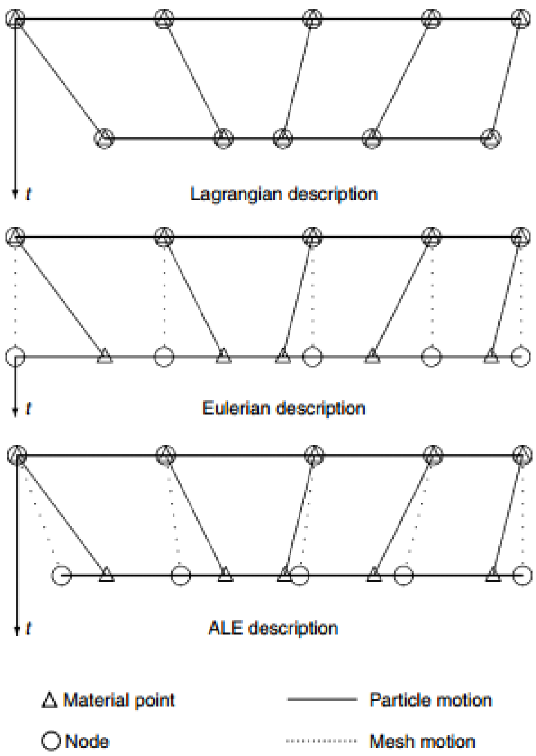

Figure 2: One-dimensional example of Lagrangian, Eulerian and ALE mesh and particle motion (Donea et al., 2004)

software, irrespective to the body motion, so that both previous formulations can be obtained as particular cases if the mesh sticks to the body or is fixed in space. However, in general, the mesh is neither Eulerian nor Lagrangian and it is managed by a procedure that tries to minimize the mesh distortions and/or concentrate the mesh in a particular regions (Donea et al., 2004).

Figure 2 shows one-dimensional example of Lagrangian, Eulerian and ALE mesh and particle motion.

In the below subsections it will be presented the mathematical formulations of the contact problem, based on the governing equations of the continuum and the Reynolds equation introduced to model the influence of the roughness on the lubricant flow in the system.

2.1 Continuum descriptions

Inspired on the studies of Hron et al. (2006) and Boman et al. (2004) some preliminary notations are of fundamental importance for the understanding of the ALE formalism.

Let **X** be the Lagrangian or material coordinate to a given material particle. The motion of this material point is described by a function denoted by φ which establishes the position of this particle as a function of time t:

$$\mathbf{x} = \boldsymbol{\varphi}(\boldsymbol{X}, t) \tag{1}$$

where **x** is the *spatial coordinate* which represent the current position of the material point **X** and φ is the function that describes the motion of this particle or the mapping function between **X** and **x** at time *t*. Thus, the material displacement is defined as:

$$\mathbf{u} = \boldsymbol{\varphi}(\boldsymbol{X}, t) - \mathbf{X}. \tag{2}$$

The motion of the continuum can be described too by a set of referential coordinates, denoted by $\boldsymbol{\chi}$. In contrast to the previous description, the motion of the referential coordinate point may not coincide with the coordinates of the material, but it is possible to establish a relation analogous to Eq. (1):

$$\mathbf{x} = \hat{\boldsymbol{\varphi}}(\boldsymbol{\chi}, t) \tag{3}$$

where $\hat{\varphi}$ is the referential motion function. Therefore, the referential displacement field is given by Eq. (4):

$$\hat{\mathbf{u}} = \hat{\boldsymbol{\varphi}}(\boldsymbol{\chi}, t) - \mathbf{X}. \tag{4}$$

The motion of the referential coordinate point can be arbitrary, but these coordinates have to be regular, so that there is a one-to-one (not always the same) relation between the current configuration $\Omega(t)$ of the body and the set of referential coordinates, represented by Ω_χ, which can be comproved by Eq. (5):

$$\hat{J} = det\hat{\mathbf{F}} \neq 0 \quad \forall \boldsymbol{\chi} \in \Omega_\chi \tag{5}$$

where

$$\hat{\mathbf{F}} = \frac{\partial \mathbf{x}}{\partial \boldsymbol{\chi}} \tag{6}$$

Similarly, the Lagrangian description in the reference configuration Ω_0 is guaranteed by the relation:

$$J = det\mathbf{F} \neq 0 \quad \forall \boldsymbol{X} \in \Omega_0 \tag{7}$$

where

$$\mathbf{F} = \frac{\partial \mathbf{x}}{\partial \boldsymbol{X}}. \tag{8}$$

Equations (5) e (7) show that for each time instant *t* there is a one-to-one relation between the referential coordinates and the material coordinates.

In describing the behavior of a continuum, the knowledge about the derivative time of some function *f* is required.

Therefore, let *f* be a function of $\mathbf{x}, \mathbf{X}$ or $\boldsymbol{\chi}$, can be defined three types of time derivatives. The spatial derivative is defined by:

$$\frac{\partial f}{\partial t} = \left.\frac{\partial f(\mathbf{x}, t)}{\partial t}\right|_{\mathbf{x}}. \tag{9}$$

The time rate of change of a quantify of a material particle is known as a material derivative and can be determined as:

$$\dot{f} = \left.\frac{\partial f(\boldsymbol{X}, t)}{\partial t}\right|_{\mathbf{X}}. \tag{10}$$

And the referential derivative is given by

$$\overset{\circ}{f} = \left.\frac{\partial f(\boldsymbol{\chi}, t)}{\partial t}\right|_{\boldsymbol{\chi}}. \tag{11}$$

Therefore, based on the above formulations, the material velocity can be expressed by

$$\boldsymbol{v} = \dot{\mathbf{x}} = \frac{\partial \boldsymbol{\varphi}(\boldsymbol{X},t)}{\partial t}, \tag{12}$$

such as the referential velocity,

$$\hat{\boldsymbol{v}} = \overset{\circ}{\boldsymbol{x}} = \frac{\partial \hat{\boldsymbol{\varphi}}(\boldsymbol{\chi}, t)}{\partial t} \tag{13}$$

The material and referential time derivative are mathematically related for any quantity f according to the following equation:

$$\dot{f} = \overset{\circ}{f} + \mathbf{c} \cdot \nabla f = \overset{\circ}{f} + c_i \frac{\partial f}{\partial x_i} \tag{14}$$

where **c** is the relative or convective velocity between the material velocity **v** and the referential velocity $\hat{\boldsymbol{v}}$, express by:

$$\boldsymbol{c} = \boldsymbol{v} - \hat{\boldsymbol{v}} \tag{15}$$

It is important to emphasize that due to the relative motion between the material and referential descriptions, the term $\boldsymbol{c} \cdot \nabla f$ in the Eq. (14) characterizes a convective effect. Since $\hat{\boldsymbol{v}}$ is arbitrary, generally the ALE formulation has no intrinsic dependence on particles or position. But, some basic considerations and/or conditions may be pointed out:

i. If $\hat{\boldsymbol{v}} = 0$, the reference system is fixed in space, wich corresponds to the Eulerian viewpoint;

ii. If $\hat{\boldsymbol{v}} = \boldsymbol{v}$, the reference system moves in space (locally) at a velocity equivalent to that of the particles, wich corresponds to the Lagrangian viewpoint;

iii. If $0 \neq \hat{\boldsymbol{v}} \neq \boldsymbol{v}$, the reference system moves in space at a arbitrary velocity and this most general case is defined as arbitrary Lagrangian-Eulerian.

2.2 Governing equations

In the Lagragian (or material) description, a transient problem defined on the domain $\Omega(t)$ bounded by $\Sigma(t)$ is mathematically modeled in the usual tensor notation as shown below:

$$\sigma_{ij,j} + \rho b_i = \rho \dot{v}_i \quad \text{in}\,\Omega(t), \tag{16}$$

where σ is the Cauchy stress tensor referent to the displacement field $\boldsymbol{u}$; $\dot{\boldsymbol{v}}$ is the material acceleration, $\boldsymbol{b}$ is the body force vector and the ρ is the mass density.

By relating the Eq. (14) and (16), we obtain the corresponding referential equation:

$$\sigma_{ij,j} + \rho b_i = \rho(\overset{\circ}{v}_i + c_j v_{i,j}) \quad \text{in } \Omega(t) \tag{17}$$

The Cauchy tensor, in Eq. (16) and Eq. (17) is obtained from the time integration of elastic-plastic large strain constitutive model.

Considering the conservation equation, to obtain her variational formulation, it is need to multiply the Eq.(17) by kinematically admissible test function $\boldsymbol{\delta u}$ over the spatial domain $\Omega(t)$, and using the divergence theorem to imbibe the traction forces on the boundary $\Sigma(t)$, we have

$$\int_\Omega \rho \delta u_i \overset{\circ}{v}_i \, d\Omega + \int_\Omega \rho \delta u_i c_j v_{i,j} \, d\Omega + \int_\Omega (\delta u_i)_{,j} \sigma_{ji} \, d\Omega = \int_\Omega \rho \delta u_i b_i \, d\Omega + \int_{\Sigma_t} \delta u_i t_i \, d\Sigma_t, \tag{18}$$

where $t_i = \sigma_{ij} n_j$ are considered the natural boundary conditions applied on Σ_t.

Therefore, we can get the discretized system of equations, substituting into Eq. (18) the following expressions:

$$\boldsymbol{u}(\boldsymbol{\chi}, t) = \sum_{i=1}^{n} \Phi_i(\boldsymbol{\chi}) u_i(t) \tag{19}$$

$$\boldsymbol{\delta u}(\boldsymbol{\chi}) = \sum_{i=1}^{n} \Phi_i(\boldsymbol{\chi}) \delta u_i \tag{20}$$

$$\boldsymbol{c}(\boldsymbol{\chi}, t) = \sum_{i=1}^{n} \Phi_i(\boldsymbol{\chi}) c_i(t) \tag{21}$$

$$\boldsymbol{v}(\boldsymbol{\chi}, t) = \sum_{i=1}^{n} \Phi_i(\boldsymbol{\chi}) v_i(t) \tag{22}$$

$$\overset{\circ}{\boldsymbol{v}}(\boldsymbol{\chi}, t) = \sum_{i=1}^{n} \Phi_i(\boldsymbol{\chi}) \overset{\circ}{v}_i(t) \tag{23}$$

$$\boldsymbol{v_0}(\boldsymbol{\chi}) = \sum_{i=1}^{n} \Phi_i(\boldsymbol{\chi}) v_{0i} \tag{24}$$

where these equations represents, respectively, mesh displacement, test functions, convective velocity, material velocity, referential acceleration and initial velocity and Φ_i are the classical FEM shape functions in which the referential coordinates $\boldsymbol{\chi}$ substitute the spatial coordinates $\boldsymbol{x}$. Equations (5) and (6) guarantees that this change of variable is regular. Then, after substitutions, the Eq. (18) can be written in simplified form, as:

$$\boldsymbol{M}\overset{\circ}{\boldsymbol{v}} + \boldsymbol{C}\boldsymbol{v} + \boldsymbol{f^{int}} = \boldsymbol{f^{ext}} \tag{25}$$

where $\boldsymbol{M}$ is the mass matrix, $\boldsymbol{C}$ the convective matrix, $\boldsymbol{f_i^{int}}$ are the internal forces and $\boldsymbol{f_i^{ext}}$ are the external applied forces and are calculated as:

$$\boldsymbol{M_{ij}} = \int_\Omega \rho \Phi_i \Phi_j \boldsymbol{I} d\Omega, \tag{26}$$

$$\boldsymbol{C_{ij}} = \int_\Omega \rho c_j \Phi_i \Phi_{j,j} \boldsymbol{I} d\Omega, \tag{27}$$

$$\boldsymbol{f_i^{int}} = \int_\Omega \boldsymbol{B_i^T} \sigma d\Omega, \tag{28}$$

$$\boldsymbol{f_i^{ext}} = \int_\Omega \rho \Phi_i \boldsymbol{b} d\Omega + \int_{\Sigma_t} \Phi_i \boldsymbol{t} d\Sigma_t, \tag{29}$$

where $\boldsymbol{I}$ is the identity matrix. For the plane strain case, for example:

$$\boldsymbol{B_i} = \begin{bmatrix} \Phi_{i,x} & 0 \\ 0 & \Phi_{i,y} \\ \Phi_{i,y} & \Phi_{i,x} \end{bmatrix} \tag{30}$$

and $\boldsymbol{I}$ is a 2×2 matrix. For both Lagrangian and ALE descriptions, the relation in Eq. (25) reduces to the quasi-static case, because the inertia forces are negligible. Therefore,

$$\boldsymbol{f_i^{int}} = \boldsymbol{f_i^{ext}} \tag{31}$$

3 LUBRICATION

3.1 Lubrication Regimes

In tribology, depending on the application and the operating conditions it is common to characterize the tribological contact by its lubrication regime (Almqvist, 2006).

Wilson (1978) introduced these different lubrication regimes, where each one of them is determined by the ratio of the lubricant film thickness (h) and the total surface roughness (R_q), and (R_t) is calculated by following expression:

$$R_t = \sqrt{R_{q1}^2 + R_{q2}^2} \tag{32}$$

where R_{q1} and R_{q2} are the mean square roughness of both surfaces in contact.

According to Montmitonnet (2001), the local lubrication regime will than be a function of Λ, with $\Lambda = h/R_t$. Therefore:

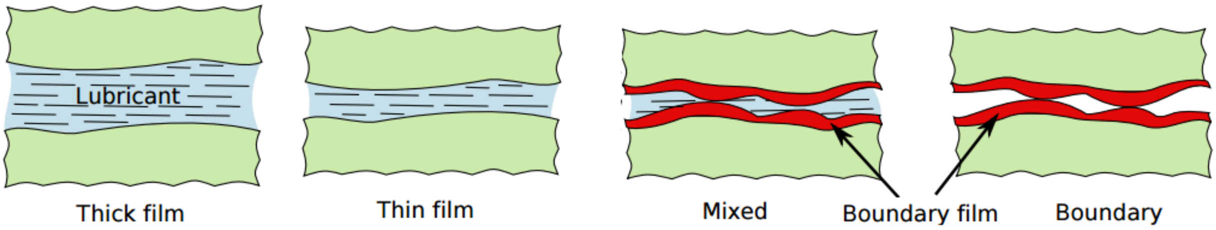

Figure 3: Lubrication regimes

i. if $\Lambda > 10$, the thick film hydrodynamic (HD) regime is identified;

ii. if $10 > \Lambda > 3$, the system is in the thin-film regime;

iii. if $3 > \Lambda > 1$, the configuration of the mixed regime is assumed;

iv. if $\Lambda < 1$, the boundary lubrication regime prevails.

The hydrodynamic action of the lubricant fluid is negligible and the load is supported intrinsically by surface asperities in the boundary lubrication regime.

The thin film regime and the thick film regime constitute the hydrodynamic regime. In a thin film mode, the surface roughness can have an important influence on the lubrication process. The contacts between individual roughness elements (asperities) carry a negligible fraction of the total load between the surfaces (Wilson, 1978), and practically no contact occurs.

In mixed lubrication analysis, some part of the pressure load is carried by asperities interactions on contact interface and the lubrication would be interrupted by contacted asperities, as illustrated in Fig. 3. In these contact regions, the friction regime is either dry contact, or boundary lubrication (a lubricant film does exist but its chemical composition is different from the bulk lubricant cant-adsorbed or chemically reacted films) or micro-HD lubrication (this means that the micro-film has the same composition as the macro-film, but two film thickness scales coexist). The rest of the load is carried by pressurized lubricant located in valleys (Boman et al., 2004).

3.2 Modeling hydrodynamic regime

In the tribological contact between rough surfaces, the films are relatively thick in the valleys of the asperities and in this case should be used the hydrodynamic lubrication (Fig. 4) theory.

In the thick film lubrication regime, the solid surface of tooling and workpiece are not in contact and the interfacial behavior is entirely determined by the lubricant film (Yang et al., 2013). So, assuming an incompressible Newtonian fluid, the Reynolds equation can be derived from the Navier-Stokes equations of fluid motion given as:

$$\begin{cases} \nabla \cdot \mathbf{v} = 0 \\ \rho \frac{d\mathbf{v}}{dt} = -\nabla p + \eta \Delta \mathbf{v} + \rho \boldsymbol{b} \end{cases} \tag{33}$$

where ρ is the density, $\boldsymbol{v}$ is the velocity, p is the pressure, η is the viscosity and $\boldsymbol{b}$ is the body force.

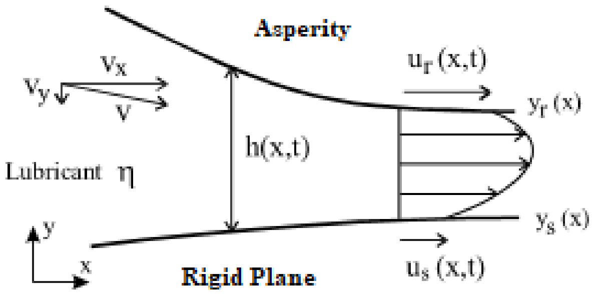

Figure 4: Hydrodynamic lubrication - the Reynolds equation (adapted from Boman et al., 2004)

However, disregarding the body forces, the inertia terms, the curvature of the film fluid (because the thickness of the lubricant is very small compared to the contact length) and assuming the smooth surfaces, the laminar flow and constants pressure and viscosity across the lubricant film, the momentum conservation equation is integrated over the thickness of the film fluid, obtaining the Reynolds equation for a 1D problem:

$$\frac{\partial}{\partial x}\left(\frac{h^3}{12\eta}\frac{\partial p}{\partial x}\right) = \frac{\partial}{\partial x}\left(\overline{u}h\right) + \frac{\partial h}{\partial t} \tag{34}$$

where $h = h(x)$ is the lubricant film thickness, $p = p(x)$ is the pressure, t is the time, $\eta = \eta(p)$ is the viscosity of the fluid, modeled by:

$$\eta(p) = \eta_0 \exp(\gamma p), \tag{35}$$

where η_0 is the viscosity at the atmosphere pressure and γ is the viscosity-pressure coefficient (m^2/N),

and $\overline{u}(x)$ is the mean velocity of the superior (u_r) and inferior (u_s) surfaces, obtained by:

$$\overline{u}(x) = \frac{(u_r + u_s)}{2}. \tag{36}$$

In the thin film hydrodynamic regime as the fluid film thickness is reduced, the asperities does not come into contact, but influence in the lubricant flow. Therefore, into the Reynolds equation it is necessary to introduce the flow factors $\phi_p(h/R_q)$ and $\phi_s(h/R_q)$, defined as pressure correction and shear correction, respectively. Then, the called average Reynolds equation modeled by Patir and Cheng (1978) is given as:

$$\frac{\partial}{\partial x}\left(\phi_p\frac{h^3}{12\eta}\frac{\partial p}{\partial x}\right) = \frac{\partial}{\partial x}\left(\overline{u}h\right) + \frac{\partial}{\partial x}\left(\frac{V}{2}R_t\phi_s\right) + \frac{\partial h}{\partial t} \tag{37}$$

where $h(x)$ and $p(x)$ are now mean local values of the film thickness and the pressure, respectively; V is the relative velocity equal to $u_r - u_s$ and R_t is obtained in Eq. (32). Thus we also have the shear stress equation for thin film regime:

$$\tau = \eta\,\frac{V}{h}\left(\phi_f \pm \phi_{fs}\right) \pm \frac{h}{2}\phi_{fp}\frac{\partial p}{\partial x} \tag{38}$$

in which ϕ_f, ϕ_{fs} and ϕ_{fp} are correction factors establish by Patir and Cheng (1978). Analogously the shear stress for the thick film regime can be calculated by:

$$\tau = \eta\,\frac{V}{h} \pm \frac{h}{2}\frac{\partial p}{\partial x}. \tag{39}$$

3.3 Modeling Mixed Lubrication

A good model for the mixed lubrication regime must combine considerations of the completely different types of processes active at the asperity valleys and peaks (Wilson, 1978).

The model proposed in this work constitutes the evaluation of the contact between main roughness and a rigid plane in order to verify the influence of the lubricant fluid in the system.

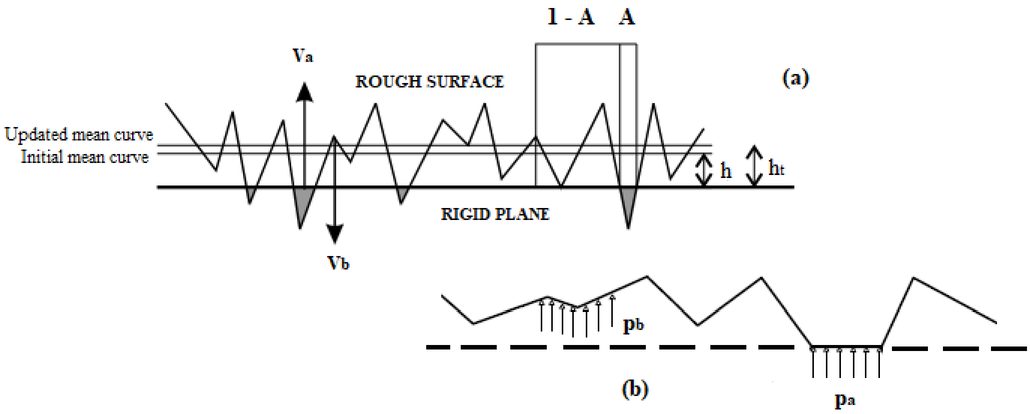

Figure 5: (a) Definition of the real area of contact and (b) Mixed lubrication regime (adapted from Boman et al., 2004)

Therefore, we use the equations that describe this regime, based on the studies of Boman et al. (2004) and Gu et al. (2016). In this case they describe that some tops of asperities are in contact and the total pressure (p) which is a result from the contact algorithm of the FEM analysis at the macroscopic level is shared at the micro-level between the hydrodynamic pressure of the lubricant (p_b), which is constrained to flow in the asperity valleys, and the asperity contact pressure (p_a):

$$p(x) = A(x)p_a(x) + (1 - A(x))p_b(x) \tag{40}$$

where $A \in [0, 1]$ is defined as the pondering factor which represents the real fractional area of contact and depends on the load carried between the elements in contact (see Fig. 5).

For this study, it is necessary to know the actual area of contact between the surfaces, which is a function of surface texture, the properties of materials and interfacial conditions of loading. This area change across the process, and consequently the mean height of the asperities too. For this reason, the mean film thickness can not be directly measured. A solution is to update the mean curve of heights of the asperities.

In the Fig. 5, at any step t the thickness measured from this updated curve is the real mean thickness h_t in comparison to the measured thickness from the initial curve h, and is very important to calculate the value of A.

The total shear stress (τ) is defined as

$$\tau(x) = A(x)\tau_a(x) + (1 - A(x))\tau_b(x) \tag{41}$$

where τ_a is the shear stress presents on the top of the asperities in contact and τ_b is the shear stress relative to the lubricant viscosity.

4 NUMERICAL MODEL

The ALE method is only implemented in Abaqus/ Explicit V6.13 as a 3D problem, because the Eulerian elements must be three-dimensional. From a general viewpoint, thats type of model constitutes in an Eulerian mesh which represents the volume in which the Eulerian material flows and interacts with Lagrangian parts of the system.

The model is created using three parts. An Eulerian part represents the domain within which the water will flow. The Lagrangian parts represents the rough surface and the rigid plane.

In the initial configuration of the model, water is located in the Eulerian part, in a region predefined (which corresponds to the lubricant film thickness). Therefore, it is to necessary to create a partition and use a tool called Eulerian Volume Fraction (EVF). This tool is used to visualize the progression of the film fluid within the Eulerian mesh.

At the beginning of a ALE simulation, a fraction of the Eulerian mesh is usually filled with material, while the rest contains void. During the computation, the EVF is tracked for each element of the Eulerian mesh (Ducobu et al., 2016).

To facilitate the calculation, it is recommended by the Abaqus User's Manual (2010) that the lagrangean parts be within the Eulerian domain at the beginning of the simulation. Moreover, the "control volume" (Eulerian domain) should be large enough to prevent the Eulerian material to flow out of it, since the simulation can be lost.

Figure 6 presents the model geometry. All created parts have depth equal to $1\,m$. The water

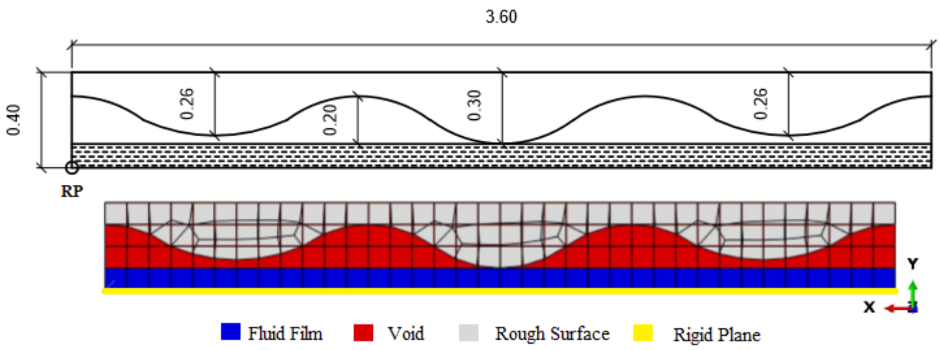

Figure 6: Model Geometry (dimensions in m)

is modeled as a nearly incompressible and viscous Newtonian fluid. The linear Hugoniot form of the Mie-Grüneisen equation of state is used in the material model. The parameters used to define the material are density (ρ) of $1000\,kg/m^3$, viscosity (η) of $0.001\,Ns/m^2$, the speed of sound c_0 equal to $1500\,m/s$, the slope of $U_s - U_p$ curve (s) = 0 and the Grüneisen ratio (Γ_0) = 0 (Abaqus User's Manual, 2010).

The solid homogeneous which represents the peaks or asperities is modeled as an elastic material with Young's modulus of $1.2 \times 10^7\ N/m^2$, Poisson's ratio of 0.4, and density of $1100\,kg/m^3$.

The rigid plane is modeled as an 3D analytic rigid shell, where material properties are not assigned.

The Eulerian part is meshed with EC3D8R (hexahedral) elements using an approximate global mesh size of 0.07. The asperities are meshed with C3D8R (hexahedral) elements of global mesh size of 0.04 and the contact region the mesh was refined with element of size equals 0.007. The values of the mesh size was obtained from a mesh convergence analysis (Fig. 7), in which the number of elements used in the mesh of the solid part representing the roughness and the maximum tangential stress resulting in the final analysis time were evaluated, for the mixed lubrication model (confined fluid). Thus, for the Eulerian part and the asperities, 3570 and 71786 hexahedral elements were used, respectively.

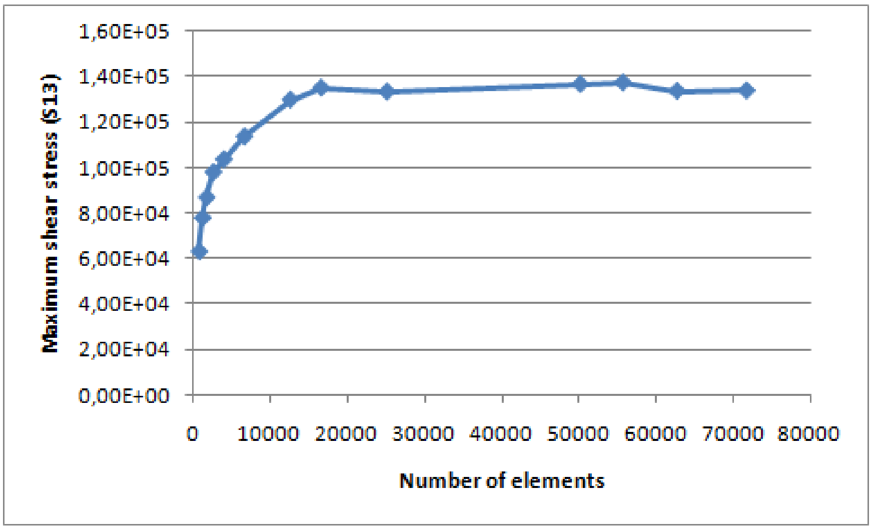

Figure 7: Convergence analysis of the mesh

In this paper are studied two conditions: in the first, the fluid flows out of the Eulerian domain and exerts no influence on the tribological system, since it does not constitute a lubrication regime because there is no confinement of the lubricating film. The second condition consists in the confinement of the fluid, and with base in the studied references the mixed lubrication regime prevails, with following considerations: in the valleys the thick film hydrodynamic regime is identified and on the peaks is defined the boundary regime.

In this model two steps are created for simulation. The first is of roughness relative to the rigid plane, and the second relative to sliding between them.

In the initial step for simulation, zero-velocity boundary conditions are applied in both conditions as detailed in the Fig. 8. However, when there is no confinement (to the free-fluid condition), V_{domain} in x and z - directions are supressed.

The boundary condition is applied in rigid plane (V_{rp}) through the reference point (RP). The velocity imposed on the roughnesses $(V_{roughsurface})$ is modified to $-0.12\,m/s$ (y-direction) so that they come into contact with the rigid plane in a period of $1\,s$ (first step); and the relative sliding velocity $(V_{roughsurface})$ is modified to $0.1\,m/s$ (z-direction), defined in a simulation period of $1\,s$ (second step). One boundary condition is imposed in the faces of the rough surfaces in x-direction, restricting any "displacements" in this direction. The velocity applied is small, theoretically ensuring that the problem is quasi-static. In the initial step, the void area corresponds to $0.35\,m^2$, which justifies the choice of a fluid film thickness of $0.1\,m$, which guarantees the confinement of this fluid at the end of the step referring to normal contact.

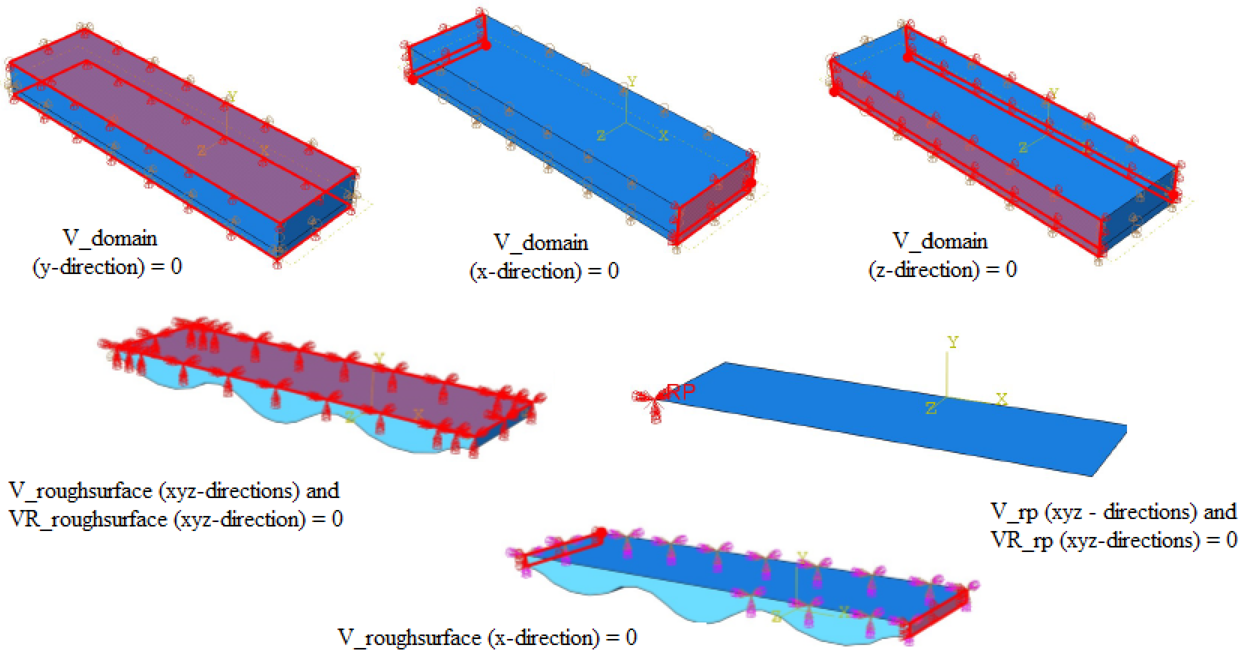

Figure 8: Boundary conditions of the model

A frictionless and hard general contact definition enforces contact between the elements of the system, for the tangential and normal behavior, respectively and a gravitational load is applied to the whole model, with value set as $9.81\,m/s^2$.

In order to evaluate the result in elements of the model in terms of tangential stress and normal stress, it is necessary to define these elements prior to the simulation, as is done for the elements contained in the region where the boundary film prevails during the slip (as demonstrated in the Fig. 9.

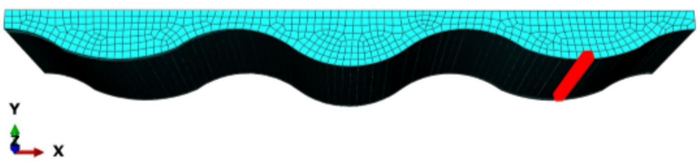

Figure 9: Elements analyzed of the rough surface mesh

The penalty contact algorithm is used in Abaqus to handle contact in ALE analysis.

5 RESULTS AND ANALYSIS

The results presented here consider the simulation from 1 second, which corresponds to the end of the step that generates the contact of the central asperity with the rigid plane and the sliding of the rough surface up to 2 seconds (final analysis time).

For the free fluid condition, the fluid flows out of the domain even before contact occurs, and as a consequence, the lubricant does not influence the tribological behavior of the rough surface at all, which can only be visualized in the confined fluid condition.

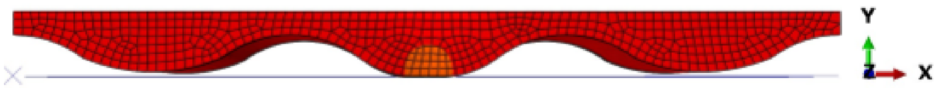

Figure 10: Displacement in 1 s

Figure 10 shows the position of the rough surface relative to the rigid plane after this initial second. Contact occurs about 0.85 seconds only in the central asperity, and the others are subjected to only pressure of the lubricating fluid (region characterized by a boundary film).

Therefore, it was sought to evaluate the shear (S_{13}) and normal (S_{22}) stresses em only in the interval of time in which the lubrication is expected to cause significant effect.

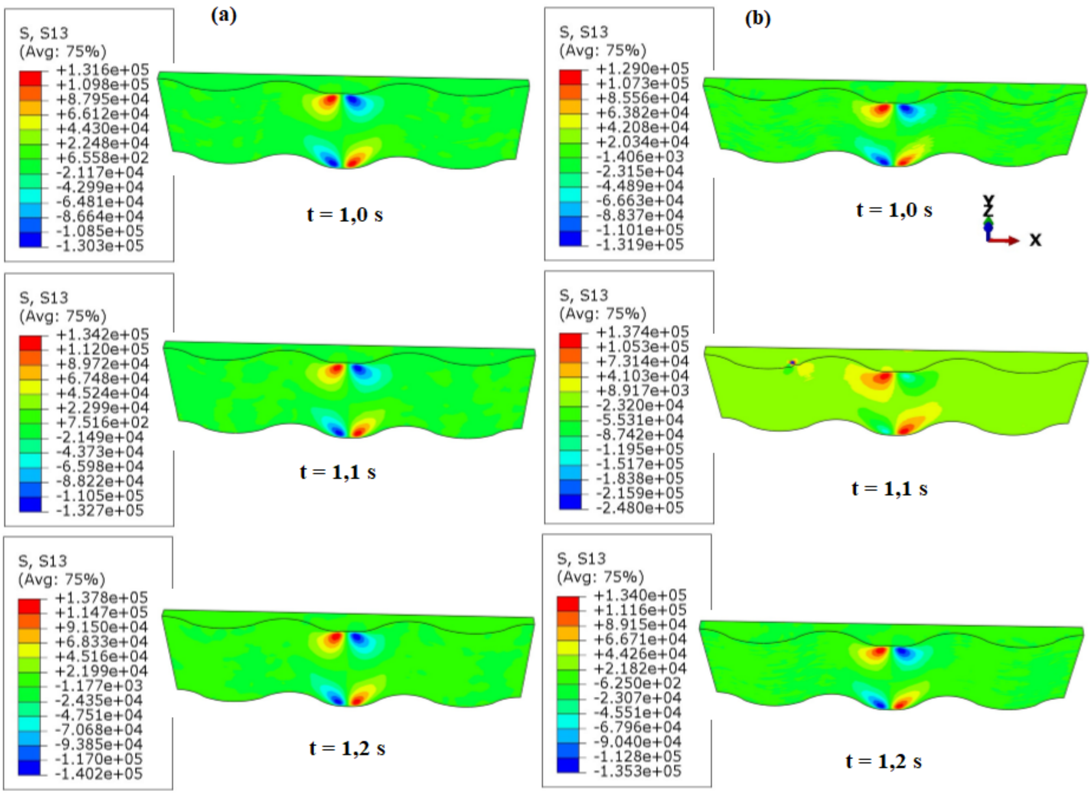

Figure 11: Shear Stress (S_{13}) em N/m^2 for (a) free fluid and (b) confined fluid

For the positive shear stress in the central asperity it is possible to identify that, the lubricated condition presents values lower than the non-lubricated system (for the free fluid condition) as can be seen in Fig. 11.

It should be noted that the negative shear stress, responsible for a considerable portion of the contact effect at the peak-plane interface, presents higher values for the lubricated system when compared to the non-lubricated system (up to 1.1 seconds) and in later seconds this result is reversed .

This would appear to indicate that in the slip phase the lubrication conditions interfere in the behavior of the rough surface, relieving the existing contact.

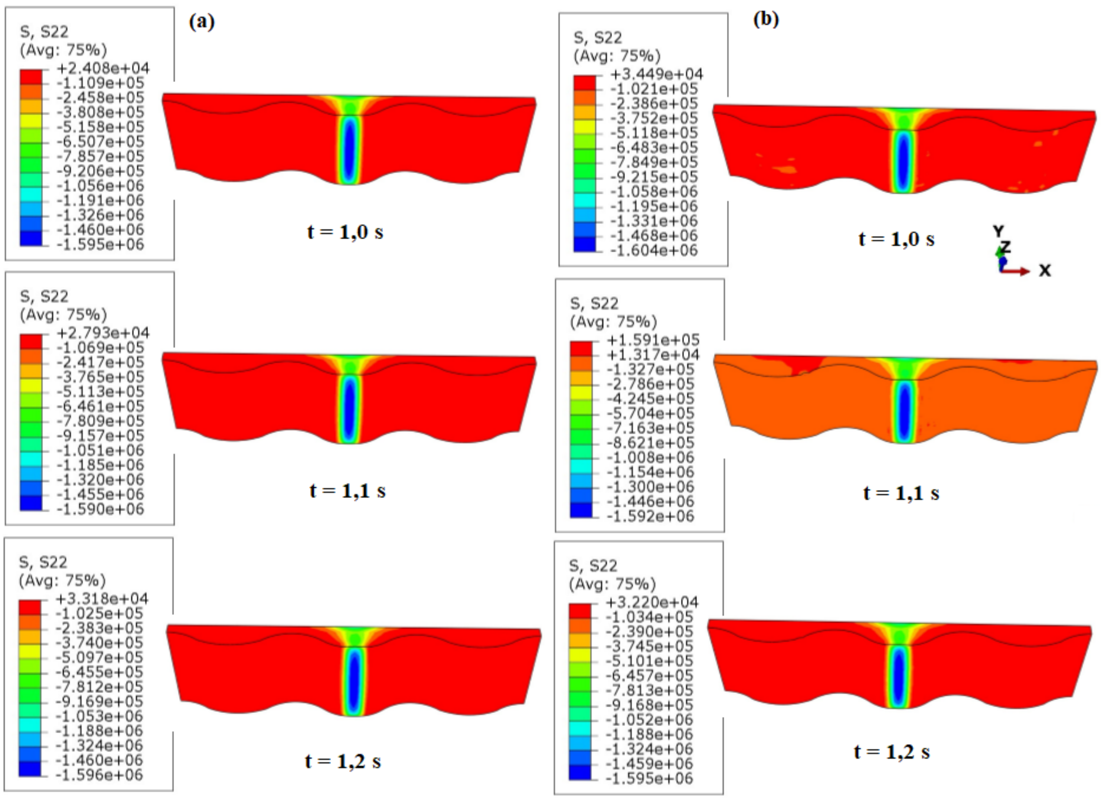

Figure 12: Normal Stress (S_{22}) em N/m^2 for (a) free fluid and (b) confined fluid

For normal stress (Fig. 12) it is not possible to identify a predefined pattern. However, up to 1.0 seconds, the traction stresses are smaller for the non-lubricated model. It is worthwhile noting that these results were evaluated for the model as a whole, mainly for the contact interface in which the stress bulb can be visualized with more emphasis.

However, there is no boundary film in the evaluated interface. Thus, it would be more interesting to analyze some elements located at the peak of asperity (Fig. 9) of smaller radius, since in these the contact does not prevail, but the boundary film is present.

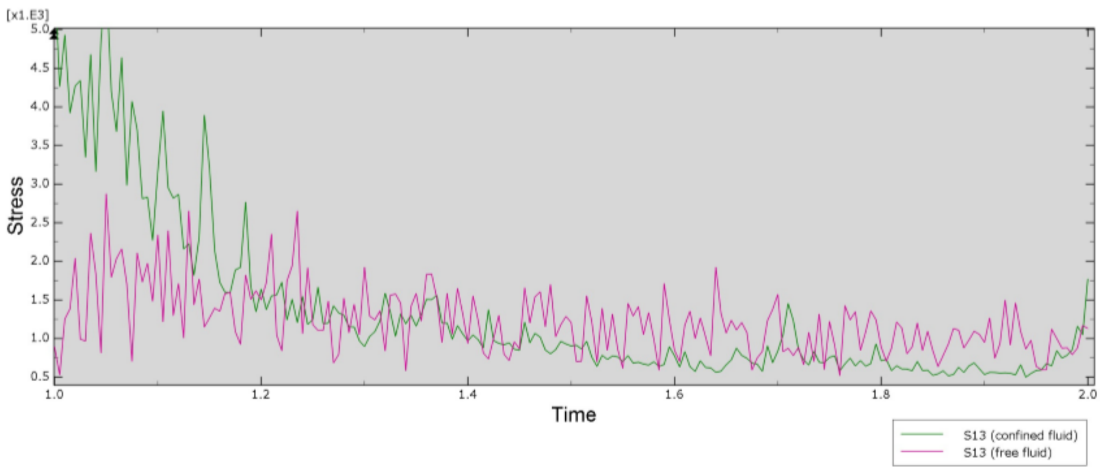

Figure 13: Shear Stress (S_{13}) em N/m^2 for free fluid and confined fluid

For these elements, the resulting average shear and normal stresses and a ratio between them (specified below) were evaluated.

For the mixed lubrication condition (confined lubricant), the shear stress (absolute average) initial to the slip is higher compared to the non-lubricated regime. However, after 1.2 seconds the result is reversed (as demonstrated in Fig. 13), which can be justified by the presence of the lubricant, since to start the slip a significant resistance is required, referring to the static friction force.

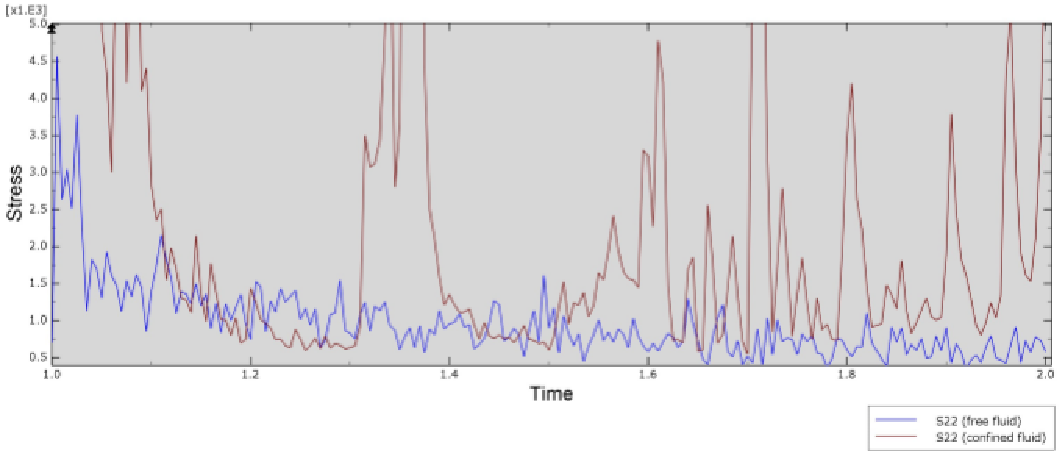

Figure 14: Normal Stress (S_{22}) em N/m^2 for free fluid and confined fluid

Considering the evolution of absolute average normal stress in both models, it is observed that in Fig. 14 the stress values in confined model are relatively high (about 5 times) in relation to the values shown for the case of free fluid. This can be attributed to the pressure the lubricant exerts on the whole system when confined.

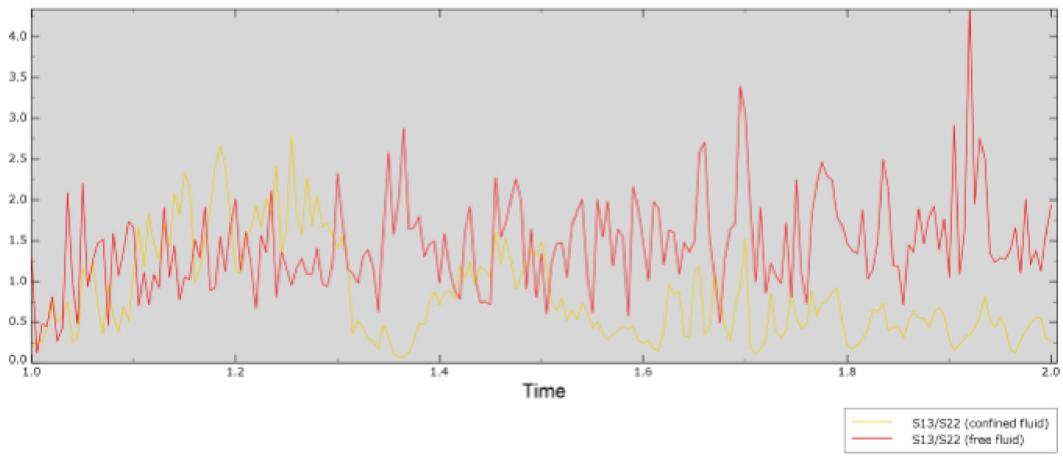

Figure 15: S_{13}/S_{22}

Assuming the ratio between shear stresses and normal stresses, the results in Fig. 15 for the free and confined fluid are obtained along the slide.

It is identified that this ratio stands out more for the non-lubricated condition.

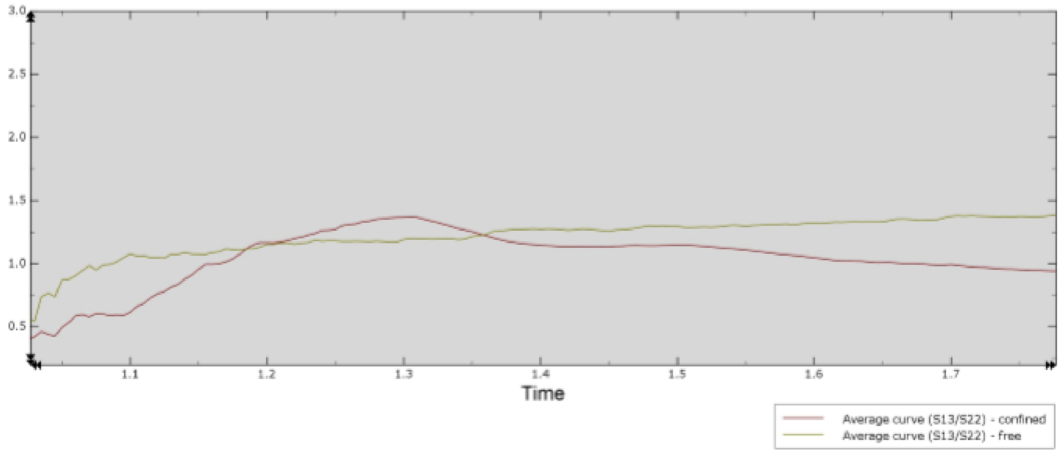

Figure 16: Average Curve (S_{13}/S_{22})

An average line can be drawn along the curves of the Fig. 16. Thus, it is possible to establish an average value for the ratio between the analyzed variables.

The result obtained confirms what was expected. At the beginning of the sliding process this ratio is smaller for the case where lubrication prevails in the system. On the other hand, in the development of this process and in function of the simulation, this relation increases and and reduces again until the end of the analysis.

Similarly, it is observed that for the case where the fluid is free to flow, this ratio occurs in a smaller proportion, but grows considerably until reaching a constant level.

Again, the static friction force responsible for initiating the sliding can be considered a prime factor that justifies the behavior of the asperities in the lubricated contact.

6 CONCLUSION

Results presented in this study showed clearly the potential of presented approach. Although its development is in an early phase, it provides a modeling of the physical the behavior of mixed lubrication by means of the finite element method, in wich it was possible to evaluate the influence of the presence of lubricant in a tribological system.

For future studies, it is worthwhile to include other configurations for the model, so that the contact occurs not between asperities and any rigid plane, but between two distinct rough surfaces, in order to identify for each configuration a lubrication regime among those presented in this work. Therefore, the contact may occur between the peaks and valleys of the surface considered.

It would be interesting to obtain the results in function of the generated contact forces, since from this one could calculate the coefficient of friction for each surface studied.

And finally, test the models for other fluids with properties of different materials, including oil and air, to verify changes in results. This is an important issue for future research.

Despite being a qualitative and hypothetical model that does not take into account the real dimension of the surface, the proposed methodology emerges as an effective alternative in the field of tribology, in the prediction of the coefficient of friction and other variables pertinent to the study of the lubricated contact.

ACKNOWLEDGMENTS

The authors would like to thank UFJF, CAPES, FAPEMIG and CNPq for supporting the development of this research.

REFERENCES

Abaqus, A., 2010. 6.11-3 Standard User Manual, ABAQUS. *Inc*, USA.

Almqvist, A. (2006). *On the effects of surface roughness in lubrication*. Doctoral dissertation, Lulea tekniska universitet.

Bastos, F. S., Ferraz, M. V. S. & Vecchio, S. D., 2017. Interação fluido-estrutura em modelo de contato lubrificado entre aspereza e plano rgido. *Revista Interdisciplinar de Pesquisa em Engenharia-RIPE*, vol. 2, n. 35, pp. 257.

Boman, R., & Ponthot, J. P., 2004. Finite element simulation of lubricated contact in rolling using the arbitrary LagrangianEulerian formulation. *Computer methods in applied mechanics and engineering*, vol. 193, n. 39, pp. 4323.

Bowden, F. P., & Tabor, D., 2001. *The friction and lubrication of solids*. Oxford university press.

Donea, J., Huerta, A., Ponthot, J. P., & Rodriguez-Ferran, A., 2004. *Encyclopedia of Computational Mechanics*. John Wiley.

Ducobu, F., Rivire-Lorphvre, E., & Filippi, E., 2016. Application of the Coupled Eulerian-Lagrangian (CEL) method to the modeling of orthogonal cutting. *European Journal of Mechanics-A/Solids*, vol. 59, pp. 58.

Gu, C., Meng, X., Xie, Y., & Zhang, D., 2016. Mixed lubrication problems in the presence of textures: An efficient solution to the cavitation problem with consideration of roughness effects. *Tribology International*, vol. 103, pp. 516.

Hron, J., & Turek, S., 2006. A monolithic FEM/multigrid solver for an ALE formulation of fluid-structure interaction with applications in biomechanics. *Fluid-structure interaction*, pp. 146.

Hua, D. Y., Qiu, L., & Cheng, H. S., 1997. Modeling of lubrication in micro contact. *Tribology Letters*, vol. 3, n. 1, pp. 81.

Khatri, C. B., & Sharma, S. C., 2016. Influence of textured surface on the performance of non-recessed hybrid journal bearing operating with non-Newtonian lubricant. *Tribology International*, vol. 95, pp. 221.

Kijima, H., & Bay, N., 2009. Influence of tool roughness and lubrication on contact conditions in skin-pass rolling. *Journal of Materials Processing Technology*, vol. 209, n. 10, pp. 4835.

Lorentz, B., 2013. *An approach to investigate surface roughness influence on non-lubricated and lubricated contacts by means of the finite element analysis*. Doctoral dissertation, Zugl.: Karlsruhe, Karlsruher Institut fr Technologie (KIT).

Montmitonnet, P., 2001. Plasto-hydrodynamic lubrication (PHD)application of lubrication theory to metal forming processes. *Comptes Rendus de l'Acadmie des Sciences-Series IV-Physics*, vol. 2, n. 5, pp. 729.

Patir, N., & Cheng, H. S., 1978. An average flow model for determining effects of three-dimensional roughness on partial hydrodynamic lubrication. *Journal of lubrication Technology*, vol. 100, n. 1, pp. 12.

Qiu, G., Henke, S., & Grabe, J., 2011. Application of a Coupled EulerianLagrangian approach on geomechanical problems involving large deformations. *Computers and Geotechnics*, vol. 38, n. 1, pp. 30.

Quiõnez, A. F., & Morales-Espejel, G. E., 2016. Surface roughness effects in hydrodynamic bearings. *Tribology International*, vol. 98, pp. 212.

Sanches, R. A. K. 2006. *Análise bidimensional de interação fluido-estrutura: desenvolvimento de código computacional*. Doctoral dissertation, Universidade de São Paulo.

Wilson, W. R. D., 1978. Friction and lubrication in bulk metal-forming processes. *Journal of Applied Metalworking*, vol. 1, n. 1, pp. 7.

Yang, T. S., & Lo, S. W., 2004. A finite element analysis of full film lubricated metal forming process. *Tribology international*, vol. 37, n. 8, pp. 591.

Zhou, Y., Chen, X., & Chen, H., 2016. A hybrid approach to the numerical solution of air flow field in aerostatic thrust bearings. *Tribology International*, vol. 102, pp. 444.